Integrating Genetic Linkage Maps With Pachytene Chromosome Structure in Maize

Lorinda K. Anderson,*[,1] Naser Salameh,[†] Hank W. Bass,[‡] Lisa C. Harper,[§] W. Z. Cande,[§] Gerd Weber[†] and Stephen M. Stack*

**Department of Biology, Colorado State University, Fort Collins, Colorado 80523, [†]Department of Plant Breeding and Biotechnology, University of Hohenheim, D-70593 Stuttgart, Germany, [‡]Department of Biological Science, Florida State University, Tallahassee, Florida 32306 and [§]Department of Molecular and Cell Biology, University of California, Berkeley, California 94720*

Manuscript received November 4, 2003
Accepted for publication January 9, 2004

ABSTRACT

Genetic linkage maps reveal the order of markers based on the frequency of recombination between markers during meiosis. Because the rate of recombination varies along chromosomes, it has been difficult to relate linkage maps to chromosome structure. Here we use cytological maps of crossing over based on recombination nodules (RNs) to predict the physical position of genetic markers on each of the 10 chromosomes of maize. This is possible because (1) all 10 maize chromosomes can be individually identified from spreads of synaptonemal complexes, (2) each RN corresponds to one crossover, and (3) the frequency of RNs on defined chromosomal segments can be converted to centimorgan values. We tested our predictions for chromosome 9 using seven genetically mapped, single-copy markers that were independently mapped on pachytene chromosomes using *in situ* hybridization. The correlation between predicted and observed locations was very strong ($r^2 = 0.996$), indicating a virtual 1:1 correspondence. Thus, this new, high-resolution, cytogenetic map enables one to predict the chromosomal location of any genetically mapped marker in maize with a high degree of accuracy. This novel approach can be applied to other organisms as well.

INTEGRATING genetic linkage maps with chromosome structure has been an important objective ever since it was demonstrated that genes occur in a fixed order on chromosomes (Sutton 1903; Bridges 1916). Linkage maps are defined by the percentage of recombination between markers [as expressed in centimorgans (cM)] and reveal the linear order of markers. However, they do not contain information on the actual physical distance between markers, whether that distance is expressed as a cytological length (positions on chromosomes) or as a physical length (number of DNA base pairs). This is because crossing over is not evenly distributed along chromosomes. Crossing over is suppressed in heterochromatin and centromeres, and crossing over is variable even in euchromatin where most crossing over occurs (Sherman and Stack 1995; Harper and Cande 2000; Anderson *et al.* 2003). As a result, linkage maps cannot be simply overlaid on chromosomes to determine the physical position of genes. Even detailed information on the linear order of genes from a complete genome sequence cannot bridge the gap between linkage maps and chromosomes because DNA (as well as crossing over) is not evenly distributed along specially organized meiotic chromosomes. This is an important point because the observed location of a gene on a chromosome (relative to the centromere) can be different on mitotic compared to meiotic chromosomes, as demonstrated by Froenicke *et al.* (2002) for mouse chromosomes. Related observations indicate that differences in mitotic and meiotic chromosomes may affect the relative cytological distance between markers in plants as well (Stack 1984). In this regard, *Drosophila melanogaster* has the best integration of cytological (chromosome), genetic (recombination), and physical (DNA sequence) aspects of the genome, but this integration is based on somatic polytene chromosomes (http://flybase.bio.indiana.edu/), not on meiotic chromosomes where crossing over actually occurs. For these reasons, the position of individual genes along meiotic chromosomes and the relation of gene position to meiotic recombination are understood only in general terms for most organisms.

Here we relate linkage maps to meiotic chromosome structure in maize by using the distribution of cytologically visible markers of crossing over called late recombination nodules (RNs) on individually identified pachytene chromosomes (Anderson *et al.* 2003). RNs are proteinaceous, multicomponent, ellipsoids ~100 nm in diameter that are found in the central region of synaptonemal complexes (SCs) between homologous chromosomes (bivalents) at pachytene (Zickler and Kleckner

[1]*Corresponding author:* Department of Biology, Colorado State University, Fort Collins, Colorado 80523.
E-mail: lorinda.anderson@colostate.edu

1999). Evidence that RNs mark crossover sites include the close correspondence between the frequency and distribution of RNs compared to chiasmata (*e.g.*, Carpenter 1979; Anderson *et al.* 2003), the presence of an essential crossover protein (MLH1p) in RNs (Moens *et al.* 2002), and the presence of MLH1p/RNs at chiasma sites (Marcon and Moens 2003). Because RNs can be observed only by electron microscopy of SCs in elongate pachytene bivalents, RNs represent the highest resolution markers available for determining the chromosomal location of crossing over. Each RN represents one crossover (equivalent to 50 cM on a linkage map), so the frequency and distribution of RNs can be used to prepare a detailed map of recombination along the physical length of each of the 10 pachytene chromosomes/SCs in maize (Anderson *et al.* 2003). Because RN maps relate the amount of recombination to cytological position along pachytene chromosomes and linkage maps report the amount of recombination relative to genes or other markers, it is now possible to combine these two approaches to directly relate genetically mapped markers to cytological position. Here, we use our RN maps to predict the cytological location of selected linkage map markers on each maize chromosome. The predicted locations of seven markers on chromosome 9 were tested using *in situ* hybridization (ISH) of single-copy DNA sequences. The predicted and observed locations of the markers on chromosome/SC 9 were highly correlated, indicating a virtual 1:1 match. From this we conclude that high-resolution RN maps can be used to accurately predict the cytological location of any genetically mapped marker.

MATERIALS AND METHODS

Preparing recombination maps on pachytene bivalents: Using SC spreads from the inbred strain KYS, the locations of centromeres and RNs were measured on each of the 10 maize pachytene bivalents (Anderson *et al.* 2003). Briefly, a standard SC karyotype was developed in which each SC was identified by relative length and arm ratio. This SC karyotype is very similar to karyotypes developed from pachytene chromosome squashes. Using the SC karyotype and an average measured length of 331 μm for a complete set of SCs, the average absolute length of each SC arm was established to the nearest 0.1 μm. The locations of RNs on identified SCs were determined as percentages of the arm length from the centromeres, and these values were then converted to absolute positions in micrometers on each of the 10 standardized SCs. The locations of 4267 RNs on 2080 individually identified SCs from 47 plants were compiled in 0.2-μm intervals (Anderson *et al.* 2003). SC lengths that were not evenly divisible by 2 (SCs 3, 5, 6, 8, 9, and 10) have one larger 0.3-μm SC segment nearest the centromere in either the short or the long arm. One RN represents a crossover between two homologous, nonsister chromatids, which yields two recombinant and two parental chromatids for a recombination frequency of 50% (or 50 cM). On this basis, RN frequency was converted to centimorgans by multiplying the number of RNs in each 0.2-μm SC segment by 50 cM and then dividing by the number of SCs observed. For example, 7 RNs observed in a single 0.2-μm segment from a total of 193 SCs identified as SC2 would be equal to a map length of (7 RNs × 50 cM/RN) ÷ 193 SCs = 1.81 cM. This operation was performed for every 0.2-μm segment on each of the 10 maize SCs. Cumulative centimorgan maps were constructed for each bivalent by adding the centimorgan values for adjacent intervals along the length of the SC (starting from the tip of the short arm). The centimorgan RN (RN-cM) maps for all maize chromosomes are available at http://www.maizegdb.org.

Adjusting the UMC98 map to fit the cumulative RN-cM map: Because the UMC98 maize linkage maps are almost twice as long as the RN-cM maps (Anderson *et al.* 2003), it was necessary to adjust the *UMC98* marker positions proportionally to fit onto the RN-cM map. The markers were converted using the following formulas where A is centimorgan length of the short arm, B is centimorgan length of the long arm, C is centimorgan position of the centromere measured from the tip of the short arm, a is centimorgan position of a marker in the short arm, and b is centimorgan position of a marker in the long arm. Subscripts UMC98 and RN indicate origin from the UMC98 and RN-cM maps, respectively. For short arm markers $(a_{\text{UMC98}}/A_{\text{UMC98}}) \times A_{\text{RN}} = a_{\text{RN}}$. For long arm markers $\{[(b_{\text{UMC98}} - C_{\text{UMC98}})/B_{\text{UMC98}}] \times B_{\text{RN}}\} + C_{\text{RN}} = b_{\text{RN}}$. The predicted physical position of a marker in the short or long arm of a pachytene chromosome (SC position) was then determined by finding the 0.2-μm interval on the cumulative centimorgan RN map, which includes the adjusted marker position. All features used to calculate the centimorgan and SC positions for all 90 core bin markers are in the appendix.

***In situ* hybridization:** The bacterial artificial chromosome (BAC) *60.j16* (encompassing the marker *crcbr58r* with a genetic map position of 96.1 cM on chromosome 9) from Dupont was localized using procedures described by Sadder and Weber (2002). Data concerning all other markers used here have been published (Shen *et al.* 1987; Sadder *et al.* 2000; Koumbaris and Bass 2003).

RESULTS

Predicting the cytological position of genetically mapped markers: The frequency of RNs in each 0.2-μm interval for each of the 10 maize pachytene SCs was converted to a centimorgan value and then summed along the length of each SC to produce a cumulative centimorgan map based on RNs (RN-cM map) for each bivalent (Figure 1, SCs 1–10). These maps are based on the positions of 4267 RNs from 2080 individually identified SCs (Anderson *et al.* 2003). Although each bivalent has a unique pattern of RNs (and a correspondingly unique centimorgan map), all 10 SCs show the same general trends with high levels of crossing over distally on each arm and reduced crossing over proximally (near the centromeres). The number of centimorgans per 0.2-μm interval was typically 0 near the centromeres of all SCs while the maximum centimorgan value for a single distal interval ranged from 2.56 cM for SC9 to 4.85 cM for SC4.

Once the centimorgan value of each 0.2-μm interval is determined, it is possible to relate a specific genetically mapped marker to a particular position on a chromosome. Certain markers (called core bin markers) were selected by Davis *et al.* (1999) to enable different linkage maps from maize and other grasses to be related

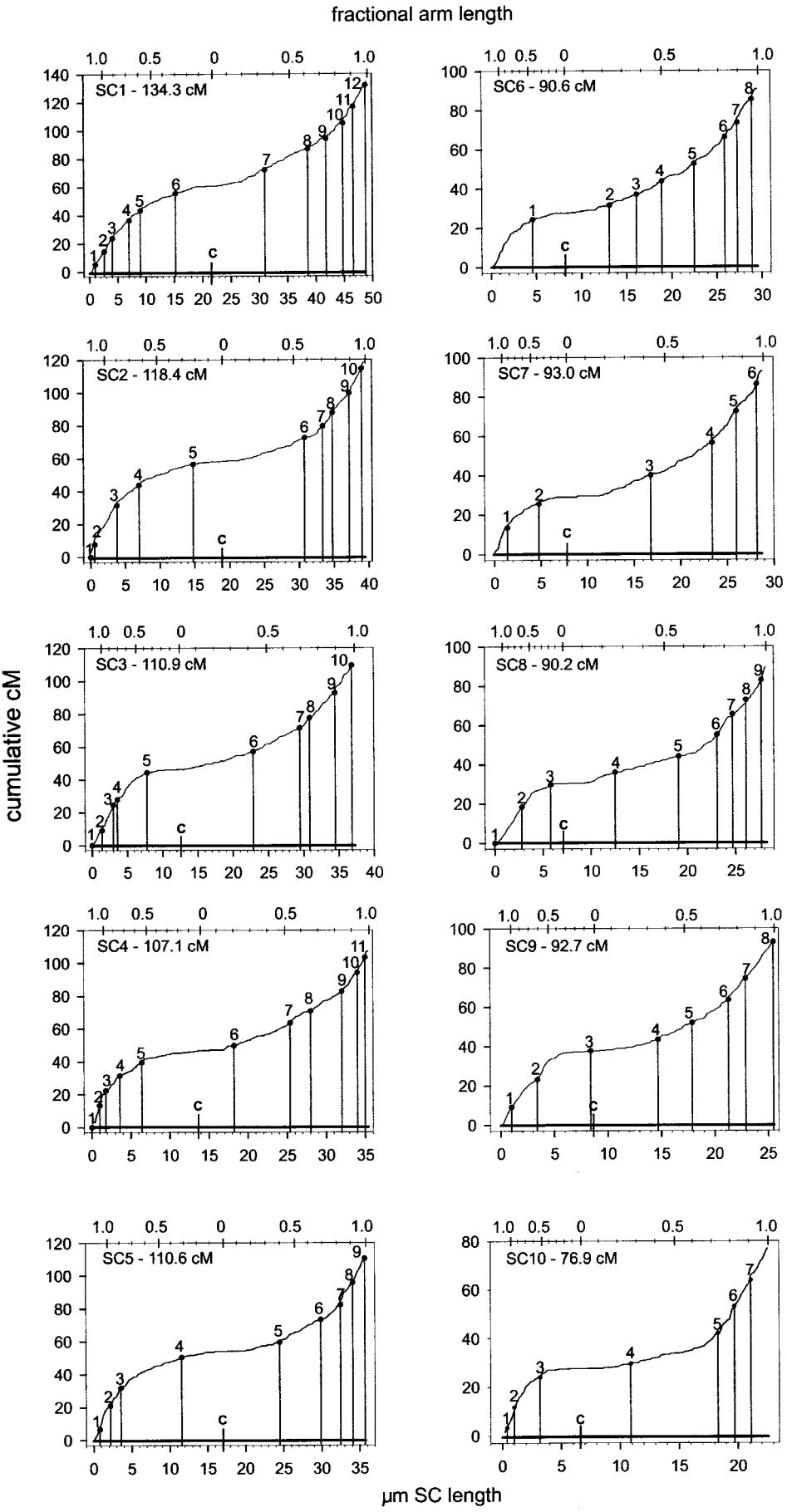

FIGURE 1.—Cumulative centimorgan maps derived from RNs, showing the distribution of crossing over along the length (in 0.2-μm intervals on the *x*-axis) for each bivalent of maize. The total map length based on RNs is given for each SC. Each SC is illustrated just above the lower *x*-axis with its short arm to the left and its centromere (C) indicated by a vertical line. On the upper *x*-axis, each SC arm has been divided into 10% length intervals. These designations are commonly used to indicate the location of translocation breakpoints. The predicted location of each core bin marker from the UMC98 map is marked by a solid circle on the cumulative centimorgan curves, and the predicted location of the marker on the chromosome/SC is indicated by a drop-down line. Core bin markers are numbered in series from the short arm to the long arm (see APPENDIX).

to one another. Core bin markers are separated by ~20 cM on each chromosome. Because of their utility and more or less even genetic spacing, we chose to map the location of these markers on the SCs. A number of different linkage maps are available for maize, but we used the UMC98 linkage map here because this map is finished, has many markers that are shared with other linkage maps, and includes the genetic locations of centromeres (http://www.maizegdb.org; Davis *et al.* 1999). For each bivalent, the UMC98 linkage map is longer, *i.e.*, more total map units, than the cumulative centimorgan RN map (Davis *et al.* 1999; Anderson *et al.* 2003), so the centimorgan value of each core bin marker was adjusted proportionally on an arm-by-arm basis to fit onto the corresponding RN map. The adjusted centimorgan value of each core bin marker was placed onto the RN-cM map to predict the physical location of each marker on the appropriate pachytene chromosome (Figure 1; SCs 1–10).

Variability in crossover rates along maize chromosomes is demonstrated by the differences in the spacing of the predicted location of core bin markers. Markers are closer to one another in distal regions that have high levels of crossing over than in proximal regions with low levels of crossing over. In some cases, the markers are spaced more or less evenly at the distal ends of arms (*e.g.*, 1S, 2L, 6L, and 8L), while in other cases, the spacing between markers is more variable (*e.g.*, 3S, 3L, and 4L). The spacing variations for core bin markers on SCs 3 and 4 are due to both differences in spacing between the markers in the UMC98 maps (with separations between markers of 5–12 cM rather than the typical 20 cM) and differences in recombination (RN) frequency along the SCs.

Predicted cytological locations of genetic markers are almost identical to cytological positions determined by *in situ* hybridization: Pachytene chromosome identification is based on squash preparations in which each bivalent can be identified by its characteristic arm ratio and relative length within the set (McClintock *et al.* 1981). These same characters can be used to accurately identify maize pachytene chromosomes in squash preparations for both ISH and SC spreads (Shen *et al.* 1987; Sadder and Weber 2002; Anderson *et al.* 2003; Koumbaris and Bass 2003). Thus, the features of pachytene chromosome structure used for identification do not change with different preparative procedures, and marker locations can be reliably compared whether RN maps on SCs or ISH markers on pachytene chromosomes are used.

We tested the predicted positions of markers on chromosome 9 using seven different single-copy sequences that have been independently mapped using ISH (Shen *et al.* 1987; Sadder *et al.* 2000; Sadder and Weber 2002; Koumbaris and Bass 2003). Each of these studies used fluorescent detection of markers except Shen *et al.* (1987) who localized the *wx1* locus using autoradiography. Nevertheless, the ISH procedure is essentially the same, and autoradiography yields results that are comparable to fluorescence *in situ* hybridization (FISH). In addition, the observed ISH position of the *wx1* locus close to the centromere in the short arm of chromosome 9 is consistent with linkage and comparative grass genome analyses (Ramakrishna *et al.* 2002). The differences between the predicted and observed chromosomal location of the sequences ranged from 0.02 μm (*wx1*) to 0.84 μm (*csu54b*; Table 1; Figure 2). These values represent differences of ~0.1 and 3.3%, respectively, of the total length of SC9. When the observed and predicted locations of the seven markers are plotted (Figure 3), the regression equation ($y = 1.01x - 0.04$, $r^2 = 0.996$) indicates a virtual 1:1 correspondence. Similar plots using the IBM2 neighbors frame 9 map (http://www.maizegdb.org; Lee *et al.* 2002) also gave an excellent correspondence between observed and predicted marker locations ($y = 0.98x + 0.62$, $r^2 = 0.996$). In comparison, the correspondence between the observed ISH positions of the markers with the predicted positions based simply on their relative (%) positions in the UMC98 linkage map is not as good ($r^2 = 0.90$), and a number of points are clearly off the regression line (Figure 3). It appears that the RN-cM map helps to fine-tune the predicted location of the markers because it corrects for differences in recombination rate along the length of chromosome 9.

Predicted genetic positions of centromeres correspond well to other estimates of centromere genetic position: It is possible that there are substantial differences in the centromere locations estimated by genetic maps and those observed on SCs (where centromeres are directly visible). To test this, we compared the genetic centromere positions from the UMC98 maps with those shown on our RN-cM maps (Table 2). The correspondence was good ($r^2 = 0.84$) with the largest difference noted for chromosome 6 that carries the nucleolar-organizing region on the short arm. With the exception of chromosome 6, the differences in centromere position are probably not great enough to have a large effect on the predicted cytological position of markers.

DISCUSSION

Integration of RN-cM maps with genetic linkage maps to predict the cytological location of markers: While a linkage map represents the linear order of markers and the frequency of recombination between markers on a chromosome, usually this map is related to the physical structure of the chromosome in only a general way. One reason for this is that the rate of recombination varies in different parts of the genome (*e.g.*, Sherman and Stack 1995; Sharopova *et al.* 2002). Thus, two markers located in a chromosomal region with a high rate of crossing over may be physically close together but separated by a comparatively large linkage map distance,

TABLE 1

Predicted and observed locations for seven markers on maize SC/chromosome 9

Marker	Symbol in Figure 2[a]	Centimorgan position: UMC98 map	Centimorgan position: Adjusted for RN map[b]	Location of marker on SC (micrometers from tip of short arm): Predicted from RN map	Location of marker on SC (micrometers from tip of short arm): Observed by ISH[c]	Difference (μm) in marker positions (% of total SC length)
umc109	1	15.5	9.1	1.0	1.8	0.8 (3.3)
bz1	2	39.3	23.1	3.4	3.1	0.4 (1.4)
umc105a	a	54.7	32.1	4.6	3.9	0.7 (2.7)
wx1	3	63.7	37.4	8.2	8.2	0.02 (0.1)
60.j16	b	96.1	58.1	20.1	20.1	0.04 (0.2)
csu145a	c	105.4	64.0	21.3	21.8	0.5 (2.0)
csu54b	8	150.4	92.7	25.5	24.7	0.8 (3.3)

[a] Core bin markers are indicated by numerals while other markers are indicated by letters.
[b] See MATERIALS AND METHODS for calculation details.
[c] Calculated from ISH marker position as a percentage of arm length.

and vice versa for markers located in regions with low rates of crossing over (*e.g.*, GILL *et al.* 1996; HARPER and CANDE 2000; KÜNZEL *et al.* 2000; SADDER and WEBER 2002; KOUMBARIS and BASS 2003).

RN-cM maps provide an opportunity to bridge the gap between linkage maps and meiotic chromosome structure. RNs are high-resolution markers of crossing over on pachytene chromosomes (ANDERSON *et al.* 2003) that can be used to directly convert linkage map position to chromosome position on the basis of crossover frequency. We used this property to predict the location of core bin markers on each of the 10 bivalents of maize. Currently, the best method available for testing our predictions in maize is by comparisons with single-copy DNA markers that have been localized to pachytene chromosomes using ISH. Since RNs and ISH markers are both mapped on pachytene chromosomes (SCs), the mapping is not influenced by inherent differences in the relative degree of chromosome condensation of euchromatin and heterochromatin. In addition, although maize chromosomes continue to contract during pachytene (GILLIES 1973), the contraction is consistent among all the chromosomes in a set and does not substantially affect arm ratio or relative length (ANDERSON *et al.* 2003). The difficulty of single-copy ISH mapping in maize limited the number of markers that were available to compare with our RN-cM predictions. Nevertheless, for chromosome 9, we were able to compare the positions of seven single-copy ISH markers with our predictions from the RN-cM map. This comparison revealed a virtual 1:1 correspondence (Figures 2 and 3). This excellent correspondence indicates that (1) pachytene chromosome structure is not changed substantially

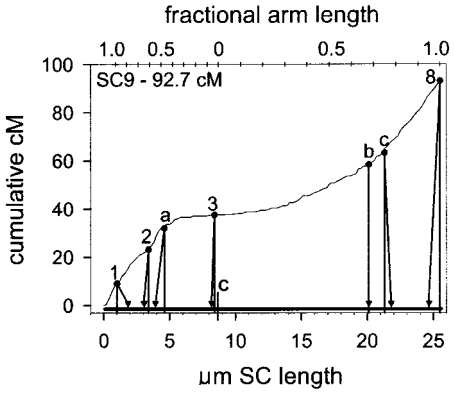

FIGURE 2.—Comparison of the predicted (solid circles on cumulative centimorgan curve and drop-down lines) and observed (by ISH, arrows) location of genetically mapped markers on maize chromosome 9 (drawn in bottom part of graph). The numbers correspond to core bin markers and the letters correspond to other genetically mapped markers that have been localized by ISH (see Table 1).

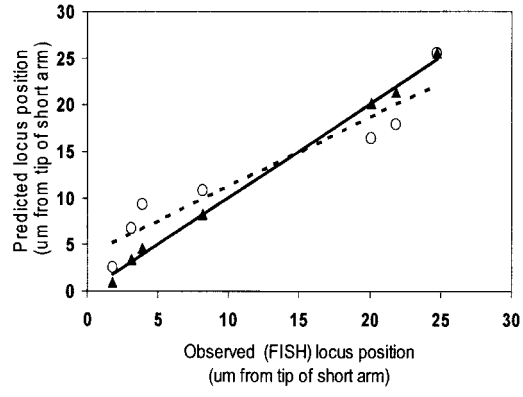

FIGURE 3.—Plots comparing observed and predicted positions of seven *UMC98* markers on maize chromosome 9. Triangles are from the RN-cM map. Open circles are from the UMC98 map with each marker expressed as a percentage of the total chromosome centimorgan map length. The predictive power of the RN map comparison ($y = 1.01x - 0.04$, $r^2 = 0.996$, solid line) is better than that of the UMC98 map comparison ($y = 0.71x + 3.88$, $r^2 = 0.900$, broken line).

TABLE 2

Comparison of centromere positions for UMC98 and RN maps

SC	Centromere position (cM)[a]		
	RN-cM map	UMC98 map[b]	Difference (%)[c]
1	60.6	66.3	5.6 (4.2)
2	58.1	53.0	5.1 (4.3)
3	46.3	47.1	0.8 (0.8)
4	46.7	44.5	2.2 (2.0)
5	53.9	58.8	4.9 (4.4)
6	27.6	13.9	13.7 (15.1)
7	28.9	30.9	2.0 (2.1)
8	30.2	24.6	5.5 (6.1)
9	37.6	39.5	1.9 (2.0)
10	27.5	33.2	5.7 (7.4)

[a] From end of short arm.
[b] Adjusted to RN-cM map.
[c] Percentage difference values are the same when using UMC98 map.

by the different procedures used for ISH and for preparing SC spreads and (2) RN-cM maps and linkage maps are closely related (even though the maps differ in overall length). Most importantly, these results demonstrate that by using these RN-cM maps it is possible to predict the cytological position of any genetic marker in maize on the basis of its map position relative to the UMC98 linkage map.

While the correspondence between the predicted and observed locations of markers for chromosome 9 is very good, it should be kept in mind that the RN-cM map is compiled from the positions of 434 RNs on 234 SCs placed onto an average SC 9 and the ISH maps are based on the average position of ISH markers similarly placed onto an average pachytene chromosome 9. Nevertheless, our results demonstrate the utility of this approach in determining the location of specific markers on maize chromosomes. In addition, the location of any marker can be individually estimated, and it is not necessary to interpolate the position of a marker of interest on the basis of its proximity to an anchored marker on a chromosome. Such interpolations can be seriously affected by variation in recombination frequency along the length of the chromosomes. Because recombination variation is directly charted by RN-cM maps, better estimates of marker position are possible.

To date, cytological and molecular maps in maize have been merged primarily using A-A and B-A translocations (Weber and Helentjaris 1989; Beckett 1991). While genetic mapping of translocation breakpoints can be precise (Beckett 1991), cytological mapping is often complicated by nonhomologous synapsis in the vicinity of the breaks that obscures the true breakpoints (Longley 1963). RN-cM maps provide a complementary approach to the use of translocations for cytological mapping, which is higher resolution and not compromised by nonhomologous synapsis. In addition, RN-cM maps supply a valuable comparison for cytological mapping using radiation hybrids (Riera-Lizarazu *et al.* 2000).

Two other studies, one in tomato and one in mouse, have combined FISH of genetically mapped markers with cytological crossover maps based on RNs and MLH1 fluorescent foci, respectively (Peterson *et al.* 1999; Froenicke *et al.* 2002). Unfortunately, Peterson *et al.* (1999) were unable to directly compare the molecular and cytological maps for three markers on chromosome 11 because the order of the markers was different in the two maps, perhaps indicating a small rearrangement in one of the tomato populations used for mapping. On the other hand, Froenicke *et al.* (2002) found a good correspondence between the position expected from the MLH1 map and the position observed by FISH for five genetically mapped markers on two mouse chromosomes. However, because each of the two chromosomes had only two or three markers for comparison, Froenicke *et al.* (2002) were not able to rigorously test the correspondence between the expected and observed positions.

Correspondence between RN-cM maps and linkage maps: The correspondence between the marker positions predicted by the RN-cM map and those observed by ISH on maize chromosome 9 is particularly striking when one considers the variables involved in the comparison. For example, the observed ISH marker locations were from four different groups using somewhat different methods. The good correspondence indicates that our RN-cM map is useful in positioning markers regardless of the source of the ISH data. Another important difference is that the UMC98 linkage map [as well as other maize linkage maps (Anderson *et al.* 2003)] is about twice as long as the RN-cM map. The reason(s) for the discrepancies in map lengths is unclear, but there are a number of differences in the procedures and populations used to generate the maps. The UMC98 linkage map is based on analysis of an immortal F_2 population of a genetic cross between two inbred lines (Tx303 and CO159; Davis *et al.* 1999) and includes both male and female recombination. In comparison, the RN-cM map is based on cytological observations of male cells from a single inbred line, KYS. Several investigators have reported differences in recombination frequency related to such variables as environmental conditions, different inbred lines, and different crosses in maize (Williams *et al.* 1995; Anderson *et al.* 2003). Other potential contributors to the differences are the type of computer program used to assemble the molecular maps and the value chosen in the computer program to indicate the strength of interference (see discussion by King *et al.* 2002). Another possibility is that the RN-cM map is too small because some RNs are lost at random. However, this is unlikely because there should be many more SCs with no RNs than are observed (Anderson *et al.* 2003). In any case, on the basis of the close correspondence

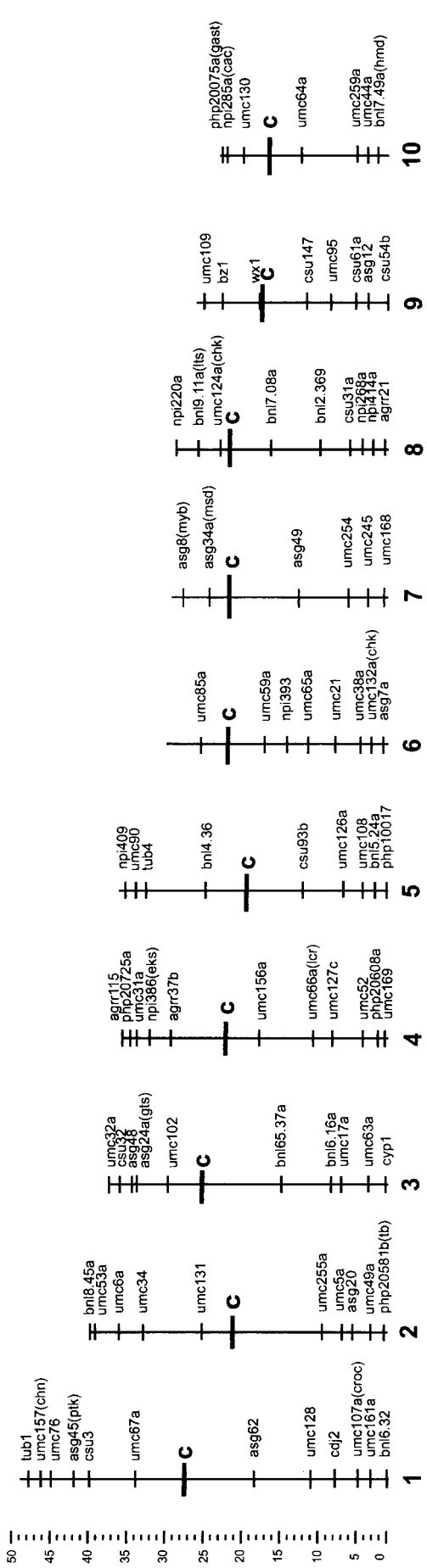

FIGURE 4.—Integrated cytogenetic map (in micrometers) of all 10 maize chromosomes/SCs with the predicted position (based on the RN-cM map for each chromosome) of core bin markers from the UMC98 linkage map. Core bin markers are rather evenly spaced genetically but not physically on the chromosomes. C, centromere.

between predicted and observed marker locations on chromosome 9, the differences between the RN-cM and linkage maps appear to be distributed proportionally along the entire length of the chromosome, at least at the resolution examined. These results also indicate that the RN-cM and the UMC98 maps are closely related measures of crossing over.

The presence of mapped centromeres in the UMC98 linkage map aided the positioning of markers on the chromosomes. This is because the low frequency of crossing over and the rather flat cumulative centimorgan map in pericentromeric regions means that resolution around centromeres is low. Indeed, when we ignored the position of the centromeres and mapped the predicted location of the seven markers on chromosome 9 from the tip of the short arm by simply multiplying their UMC map positions by the ratio of the RN-cM map length to the UMC98 map length, *wx1* mapped to the long arm (11.9 μm) rather than to the short arm (8.2 μm) where it has been located by ISH, linkage, and comparative genome analyses. In contrast, four of the other six more-distal markers changed position only slightly (0.2–0.4 μm or 0.7–1.4% of the total length of SC 9). Thus, predicting the location of markers as a function of their distance from the centromere is particularly important for markers around centromeres.

Integration of the RN-cM and linkage maps reveals that most of the linkage map (including core bin markers and genes) is located distally (Figures 1 and 4). This suggestion is also supported by the observation that genes are hot spots for recombination (CIVARDI *et al.* 1994; SCHNABLE *et al.* 1998; FU *et al.* 2001, 2002; YAO *et al.* 2002). A similar clustering of genes in distal regions of chromosomes has been reported for other cereal grains (*e.g.*, GILL *et al.* 1996).

Resolution of the RN-cM map: The resolution of the RN-cM map is based on the 1671 0.2-μm SC segments that were used for mapping. Segments this size correspond to 0.4% (SC1) to 0.9% (SC10) of pachytene chromosome length. The resolution of the maize RN-cM map in terms of DNA amount can be calculated to be ~1.6 Mbp of DNA per 0.2-μm segment (2675 Mbp per 1C DNA ÷ 1671 segments; BENNETT *et al.* 2000). However, this calculation assumes that the DNA is evenly distributed along the length of each chromosome. In tomato, heterochromatic regions of pachytene chromosomes contain about six times more DNA per micrometer of SC than do euchromatic regions (PETERSON *et al.* 1996). While the heterochromatin of maize (aside from knobs) is not as prominent as that of tomato, the amount of DNA per SC length in the more heterochromatic proximal segments of maize pachytene chromosomes (CARLSON 1988) is undoubtedly higher than the average value of 1.6 Mbp per segment, while that of the more distal, gene-rich, euchromatic regions is consequently lower than the average value. Thus, the resolution of RN-cM maps in distal regions may approach the 0.5–1.0 Mbp resolution for cytological mapping ex-

pected from radiation hybrids (Riera-Lizarazu *et al.* 2000).

In terms of centimorgans, the resolution of the RN-cM map can be calculated to average ~0.62 cM per 0.2-μm SC segment (1030 cM ÷ 1671 segments; Anderson *et al.* 2003). This calculation is an oversimplification since RN frequency varies along maize pachytene chromosomes. For example, many proximal segments have essentially 0 cM per segment while more distal segments (specifically, the most distal 3 μm of each arm) average 1.44 cM per 0.2 μm segment. Thus, distal regions of SCs where most of the genes are located tend to have both less DNA per unit SC length and at least a twofold higher crossover frequency than the genome as a whole.

Conclusion: Currently, integration of linkage maps with chromosome structure relies heavily on mapping multiple single-copy FISH markers, often on mitotic chromosomes (*e.g.*, humans, Korenberg *et al.* 1999) with more recent mapping using pachytene chromosomes (*e.g.*, rice chromosome 10, Cheng *et al.* 2001; maize chromosome 9, Sadder and Weber 2002; Koumbaris and Bass 2003). Unfortunately, single-copy FISH is particularly difficult in species such as maize that have many duplications and repetitive sequences (Sadder and Weber 2002). Here we demonstrate that the cytological crossover (RN-cM) map for maize SC 9 can be used to integrate accurately genetically mapped loci with the structure of the pachytene chromosome. On the basis of this result, it is likely that the RN-cM maps will be equally useful in predicting the location of genetically mapped markers on the other nine bivalents. Our predictions for the locations of core bin markers (as well as any genetically mapped marker) can be tested using single-copy FISH probes. Testing the predictions will require only a few selected markers for each maize chromosome, an important consideration given the difficulty in generating appropriate probes for single-copy FISH localization. This RN-cM approach is not limited to maize since RN and MLH1 foci maps are currently available for tomato (Sherman and Stack 1995) and mouse (Froenicke *et al.* 2002), and comparable maps can be prepared for other organisms (*e.g.*, humans, Lynn *et al.* 2002). RN mapping provides a bridge between cytological and genetic aspects of crossing over that will be valuable in merging genome sequence, linkage maps, and meiotic chromosome structure into a unified whole to better understand such topics as genetic interference and genome evolution in a number of different organisms (Stephan and Langley 1998; Tenaillon *et al.* 2002).

We thank M. Morgante at Dupont for kindly providing BAC *60.j16*. We also thank Terry Ashley for reading and commenting on early manuscript versions. N.S. was the recipient of a Ph.D. fellowship from the German Academic Exchange Service. This work was supported by the National Science Foundation (MCB-9728673 to S.M.S., MCB-0314644 to L.K.A., and DBI-9813365 to Z.C. and L.H.); the Consortium for Plant Biotechnology Research (DOE OR22072-102) and the Florida State University Research Foundation (to H.B.); and Eiselenstiftung, Ulm, Germany (to G.W.).

LITERATURE CITED

Anderson, L. K., G. G. Doyle, B. Brigham, J. Carter, K. D. Hooker *et al.*, 2003 High resolution crossover maps for each bivalent of *Zea mays* using recombination nodules. Genetics **165:** 849–865.

Beckett, J. B., 1991 Cytogenetic, genetic and plant breeding applications of B-A translocations in maize, pp. 493–529 in *Chromosome Engineering in Plants*, Pt. A, edited by T. Tsuchiya and P. K. Gupta. Royal Botanic Gardens, Kew, UK.

Bennett, M. D., A. V. Cox and I. J. Leitch, 2000 Angiosperm DNA *C*-values database (http://www.rbgkew.org.uk/cval/homepage.html).

Bridges, C. B., 1916 Nondisjunction as proof of the chromosome theory of heredity. Genetics **1:** 1–52.

Carlson, W. R., 1988 The cytogenetics of corn, pp. 259–331 in *Corn and Corn Improvement*, edited by G. F. Sprague and J. W. Dudley. Crop Science Society, Madison, WI.

Carpenter, A. T. C., 1979 Synaptonemal complex and recombination nodules in wild type *Drosophila melanogaster* females. Genetics **92:** 511–541.

Cheng, Z., G. G. Presting, C. R. Buell, R. A. Wing and J. Jiang, 2001 High-resolution pachytene chromosome mapping of bacterial artificial chromosomes anchored by genetic markers reveals the centromere location and the distribution of genetic recombination along chromosome 10 of rice. Genetics **157:** 1749–1757.

Civardi, L., Y. Xia, K. Edwards, P. S. Schnable and B. J. Nikolau, 1994 The relationship between genetic and physical distances in the cloned *al-sh2* interval of *Zea mays* L. genome. Proc. Natl. Acad. Sci. USA **91:** 8268–8272.

Davis, G. L., M. D. McMullen, C. Baysdorfer, T. Musket, D. Grant *et al.*, 1999 A maize map standard with sequences core markers, grass genome reference points and 932 expressed sequence tagged sites (ESTs) in a 1736-locus map. Genetics **152:** 1137–1172.

Froenicke, L., L. K. Anderson, J. Weinberg and T. Ashley, 2002 Male mouse recombination maps for each autosome identified by chromosome painting. Am. J. Hum. Genet. **71:** 1353–1368.

Fu, H., W. Park, X. Yan, Z. Zheng, B. Shen *et al.*, 2001 The highly recombinogenic *bz* locus lies in an unusually gene-rich region of the maize genome. Proc. Natl. Acad. Sci. USA **98:** 8903–8908.

Fu, H., Z. Zheng and H. K. Dooner, 2002 Recombination rates between adjacent genic and retrotransposon regions in maize vary by 2 orders of magnitude. Proc. Natl. Acad. Sci. USA **99:** 1082–1087.

Gill, K. S., B. S. Gill, T. R. Endo and E. V. Boyko, 1996 Identification and high-density mapping of gene-rich regions in chromosome group 5 of wheat. Genetics **143:** 1001–1012.

Gillies, C. B., 1973 Ultrastructural analysis of maize pachytene karyotypes by three dimensional reconstruction of the synaptonemal complexes. Chromosoma **43:** 145–176.

Harper, L. C., and W. Z. Cande, 2000 Mapping a new frontier; development of integrated cytogenetic maps in plants. Funct. Integr. Genomics **1:** 89–98.

King, J., I. P. Roberts, M. J. Kearsey, H. M. Thomas, R. N. Jones *et al.*, 2002 A demonstration of a 1:1 correspondence between chiasma frequency and recombination using a *Lolium perenne*/*Festuca pratensis* substitution. Genetics **161:** 307–314.

Korenberg, J. R., X.-N. Chen, Z. Sun, Z.-Y. Shi, S. Ma *et al.*, 1999 Human genome anatomy: BACs integrating the genetic and cytogenetic maps for bridging genome and biomedicine. Genome Res. **9:** 994–1001.

Koumbaris, G. L., and H. W. Bass, 2003 A new single-locus cytogenetic mapping system for maize (*Zea mays* L.): overcoming FISH detection limits with marker-selected sorghum (*S. propinquum* L.) BAC clones. Plant J. **35:** 647–659.

Künzel, G., L. Korzun and A. Meister, 2000 Cytologically integrated physical restriction fragment length polymorphism maps of the barley genome based on translocation breakpoints. Genetics **154:** 397–412.

Lee, M., N. Sharopova, W. D. Beavis, D. Grant, M. Katt *et al.*, 2002 Expanding the genetic map of maize with the intermated B73 × Mo17 (*IBM*) population. Plant Mol. Biol. **48:** 453–461.

Longley, A. E., 1963 Breakage points for four corn translocation series and other corn chromosome aberrations maintained at the California Institute of Technology. USDA Crops Research ARS 34-16, Pasadena, CA.

Lynn, A., K. E. Koehler, L. Judis, E. R. Chan, J. P. Cherry *et al.*, 2002 Covariation of synaptonemal complex length and mammalian meiotic exchange rates. Science **206:** 2222–2225.

Marcon, E., and P. Moens, 2003 Mlh1p and Mlh3p localize to precociously induced chiasmata of okadaic-acid-treated mouse spermatocytes. Genetics **165:** 2283–2287.

McClintock, B., T. A. Kato and A. Blumenschein, 1981 *Chromosome Constitution of Races of Maize.* Colegio de Postgraduados, Chapingo, Mexico.

Moens, P. B., N. K. Kolas, M. Tarsounas, E. Marcon, P. E. Cohen *et al.*, 2002 The time course and chromosomal localization of recombination-related proteins at meiosis in the mouse are compatible with models that can resolve the early DNA-DNA interactions without reciprocal recombination. J. Cell Sci. **115:** 1611–1622.

Peterson, D. G., H. J. Price, J. S. Johnston and S. M. Stack, 1996 DNA content of heterochromatin and euchromatin in tomato (*Lycopersicon esculentum*) pachytene chromosomes. Genome **39:** 77–82.

Peterson, D. G., N. Lapitan and S. M. Stack, 1999 Localization of single- and low-copy sequences on tomato synaptonemal complex spreads using fluorescence *in situ* hybridization (FISH). Genetics **152:** 427–439.

Ramakrishna, W., J. Ma, P. Sanmiguel, J. Emberton, J. Dubcovsky *et al.*, 2002 Frequent genic rearrangements in two regions of grass genomes identified by comparative sequence analysis. Comp. Funct. Genomics **3:** 165–166.

Riera-Lizarazu, O., M. I. Vales, E. V. Ananiev, H. W. Rines and R. L. Phillips, 2000 Production and characterization of maize chromosome 9 radiation hybrids derived from an oat-maize addition line. Genetics **156:** 327–339.

Sadder, M. T., and G. Weber, 2002 Comparison between genetic and physical maps in *Zea mays* L. of molecular markers linked to resistance against *Diatraea* spp. Theor. Appl. Genet. **104:** 908–915.

Sadder, M. T., N. Ponelies, U. Born and G. Weber, 2000 Physical localization of single-copy sequences on pachytene chromosomes in maize (*Zea mays* L.) by chromosome *in situ* suppression hybridization. Genome **43:** 1081–1083.

Schnable, P. S., A.-P. Hsia and B. J. Nikolau, 1998 Genetic recombination in plants. Curr. Opin. Plant Biol. **1:** 123–129.

Sharopova, N., M. D. McMullen, L. Schultz, S. Schroeder, H. Sanchez-Villeda *et al.*, 2002 Development and mapping of SSR markers for maize. Plant Mol. Biol. **48:** 463–481.

Shen, D., Z. Wang and M. Wu, 1987 Gene mapping on maize pachytene chromosomes by *in situ* hybridization. Chromosoma **95:** 311–314.

Sherman, J. D., and S. M. Stack, 1995 Two-dimensional spreads of synaptonemal complexes from solanaceous plants. VI. High-resolution recombination nodule map for tomato (*Lycopersicon esculentum*). Genetics **141:** 683–708.

Stack, S. M., 1984 Heterochromatin, the synaptonemal complex, and crossing over. J. Cell Sci. **71:** 159–176.

Stephan, W., and C. H. Langley, 1998 DNA polymorphism in Lycopersicon and crossing-over per physical length. Genetics **150:** 1585–1593.

Sutton, W. S., 1903 The chromosomes in heredity. Biol. Bull. **4:** 231–248.

Tenaillon, M. I., M. C. Sawkins, L. K. Anderson, S. M. Stack, J. Doebley *et al.*, 2002 Patterns of diversity and recombination along chromosome 1 of maize (*Zea mays* sp. *mays* L.). Genetics **162:** 1401–1413.

Weber, D., and T. Helentjaris, 1989 Mapping RFLP loci in maize using B-A translocations. Genetics **121:** 583–590.

Williams, C. G., M. M. Goodman and C. W. Stuber, 1995 Comparative recombination distances among *Zea mays* L. inbreds, wide crosses and interspecific hybrids. Genetics **141:** 1573–1581.

Yao, H., Q. Zhou, J. Li, H. Smith, M. Yandeau *et al.*, 2002 Molecular characterization of meiotic recombination across the 140-kb multigenic *a1-sh2* interval of maize. Proc. Natl. Acad. Sci. USA **99:** 6157–6162.

Zickler, D., and N. Kleckner, 1999 Meiotic chromosomes: integrating structure and function. Annu. Rev. Genet. **33:** 603–754.

Communicating editor: R. S. Hawley

APPENDIX

Conversion of core bin markers from UMC98 linkage map to a predicted position on the appropriate SC

		UMC98 marker position					
Locus	Bin	Centimorgan (cM)	As fraction of cM map from centromere	Converted to RN-cM map	Corresponding absolute position on SC/chromosome[a]	Position as fractional length of arm from centromere	Arm
tub1	1.01	11.0	0.91	5.4	1.0	0.95	S
umc157(chn)	1.02	29.8	0.76	14.7	2.6	0.88	S
umc76	1.03	48.4	0.61	23.9	4.0	0.82	S
asg45(ptk)	1.04	74.0	0.40	36.5	7.0	0.68	S
csu3	1.05	88.5	0.28	43.6	9.0	0.58	S
umc67a	1.06	112.9	0.08	55.7	15.2	0.30	S
cent1	1.06	123.0	0.00	60.6	21.6	0.00	C
asg62	1.07	142.8	0.16	72.2	31.0	0.34	L
umc128	1.08	168.1	0.36	87.0	38.6	0.62	L
cdj2	1.09	180.7	0.46	94.3	41.8	0.74	L
umc107a(croc)	1.10	199.2	0.60	105.1	44.8	0.85	L
umc161a	1.11	219.3	0.76	116.8	46.6	0.91	L
bnl6.32	1.12	245.2	0.97	131.9	48.8	0.99	L
bnl8.45a	2.01	0.00	1.00	0.0	0.0	1.00	S
umc53a	2.02	12.4	0.87	7.7	0.6	0.97	S
umc6a	2.03	50.6	0.46	31.6	3.8	0.80	S
umc34	2.04	70.2	0.25	43.9	7.0	0.63	S
umc131	2.05	90.4	0.03	56.5	14.8	0.22	S
cent2	2.05	93.0	0.00	58.1	18.9	0.00	C

(*continued*)

APPENDIX

(Continued)

Locus	Bin	*UMC98* marker position: Centimorgan (cM)	*UMC98* marker position: As fraction of cM map from centromere	*UMC98* marker position: Converted to RN-cM map	Corresponding absolute position on SC/chromosome[a]	Position as fractional length of arm from centromere	Arm
Umc255a	2.06	120.3	0.24	72.5	30.8	0.58	L
umc5a	2.07	133.8	0.36	79.6	33.4	0.71	L
asg20	2.08	149.2	0.49	87.7	34.8	0.78	L
umc49a	2.09	171.9	0.69	99.6	37.2	0.89	L
php20581b(tb)	2.10	200.2	0.94	114.5	39.0	0.98	L
umc32a	3.01	0.00	1.00	0.0	0.0	1.00	S
csu32	3.02	13.9	0.80	9.1	1.4	0.89	S
asg24a(gts)	3.03	37.6	0.47	24.6	3.0	0.76	S
asg48	3.04	42.8	0.40	27.9	3.6	0.71	S
umc102	3.05	67.9	0.04	44.3	7.8	0.37	S
cent3	3.05	70.9	0.00	46.3	12.3	0.00	C
bnl65.37a	3.06	87.0	0.17	57.1	22.9	0.43	L
bnl6.16a	3.07	108.3	0.39	71.5	29.5	0.69	L
umc17a	3.08	117.5	0.49	77.7	30.9	0.75	L
umc63a	3.09	139.9	0.72	92.8	34.5	0.90	L
cyp1	3.10	164.8	0.98	109.6	36.9	0.99	L
agrr115	4.01	0.00	1.00	0.0	0.0	1.00	S
php20725a	4.02	20.9	0.71	13.5	1.0	0.93	S
umc31a	4.03	35.1	0.52	22.7	2.0	0.86	S
npi386(eks)	4.04	49.3	0.32	31.9	3.6	0.74	S
agrr37b	4.05	61.7	0.15	39.9	6.4	0.54	S
cent4	4.05	73.0	0.00	47.2	13.8	0.00	C
umc156a	4.06	78.4	0.05	50.4	18.2	0.20	L
umc66a(lcr)	4.07	101.9	0.28	64.2	25.4	0.54	
umc127c	4.08	114.0	0.40	71.3	28.0	0.66	L
umc52	4.09	134.5	0.60	83.4	32.0	0.84	L
php20608a	4.10	153.7	0.79	94.7	34.0	0.94	L
umc169	4.11	169.7	0.94	104.1	35.0	0.98	L
npi409	5.01	11.6	0.88	6.7	0.8	0.95	S
umc90	5.02	36.3	0.61	21.1	2.2	0.87	S
tub4	5.03	55.0	0.41	31.9	3.6	0.79	S
bnl4.36	5.04	86.7	0.07	50.3	11.6	0.32	S
cent5	5.04	93.0	0.00	53.9	17.0	0.00	C
csu93b	5.05	101.1	0.10	59.5	24.5	0.40	L
umc126a	5.06	121.0	0.34	73.3	29.9	0.69	L
umc108	5.07	134.0	0.50	82.3	32.5	0.83	L
bnl5.24a	5.08	153.3	0.74	95.7	34.1	0.91	L
php10017	5.09	174.8	1.00	110.6	35.7	1.00	L
umc85a	6.01	22.8	0.12	24.4	4.6	0.43	S
cent6	6.01	25.8	0.00	27.6	8.1	0.00	C
umc59a	6.02	34.7	0.06	31.5	13.1	0.23	L

(*continued*)

APPENDIX

(Continued)

Locus	Bin	*UMC98* marker position: Centimorgan (cM)	*UMC98* marker position: As fraction of cM map from centromere	*UMC98* marker position: Converted to RN-cM map	Corresponding absolute position on SC/chromosome[a]	Position as fractional length of arm from centromere	Arm
npi393	6.03	47.2	0.15	37.0	16.1	0.37	L
umc65a	6.04	62.4	0.26	43.7	18.9	0.51	L
umc21	6.05	82.6	0.40	52.6	22.5	0.67	L
umc38a	6.06	113.3	0.61	66.2	25.9	0.83	L
umc132a(chk)	6.07	129.9	0.73	73.5	27.3	0.90	L
asg7a	6.08	156.9	0.92	85.5	28.9	0.97	L
asg8(myb)	7.01	22.8	0.53	13.5	1.4	0.82	S
asg34a(msd)	7.02	43.5	0.11	25.7	4.8	0.38	S
cent7	7.02	49.0	0.00	28.9	7.7	0.00	C
asg49	7.03	66.1	0.17	40.0	16.8	0.43	L
umc254	7.04	91.5	0.43	56.6	23.4	0.74	L
umc245	7.05	116.3	0.68	72.7	26.0	0.87	L
umc168	7.06	137.5	0.90	86.5	28.2	0.97	L
npi220a	8.01	0.0	1.00	0.0	0.0	1.00	S
bnl9.11a(lts)	8.02	30.6	0.39	18.5	2.8	0.60	S
umc124a(chk)	8.03	49.3	0.01	29.7	5.8	0.17	S
cent8	8.03	50.0	0.00	30.2	7.0	0.00	C
bnl7.08a	8.04	62.9	0.10	36.0	12.5	0.26	L
bnl2.369	8.05	81.0	0.23	44.1	19.1	0.57	L
csu31a	8.06	105.5	0.42	55.2	23.1	0.76	L
npi268a	8.07	128.6	0.59	65.6	24.7	0.84	L
npi414a	8.08	144.7	0.71	72.8	26.1	0.91	L
agrr21	8.09	167.2	0.88	83.0	27.7	0.98	L
umc109	9.01	15.5	0.76	9.2	1.0	0.86	S
bz1	9.02	39.3	0.39	23.2	3.4	0.61	S
wx1	9.03	63.7	0.00	37.6	8.2	0.06	S
cent9	9.03	64.0	0.00	37.8	8.7	0.00	C
csu147	9.04	72.8	0.10	43.5	14.7	0.36	L
umc95	9.05	86.1	0.26	52.0	17.9	0.55	L
csu61a	9.06	104.4	0.47	63.7	21.3	0.75	L
asg12	9.07	121.2	0.66	74.5	22.9	0.85	
csu54b	9.08	150.4	1.00	93.2	25.5	1.00	
php20075a(gast)	10.01	7.2	0.88	3.4	0.4	0.94	S
npi285a(cac)	10.02	24.8	0.57	11.8	1.0	0.85	S
umc130	10.03	50.7	0.13	24.1	3.2	0.52	S
cent10	10.03	58.0	0.00	27.5	6.6	0.00	C
umc64a	10.04	61.0	0.04	29.5	10.9	0.27	L
umc259a	10.05	80.5	0.29	42.1	18.3	0.74	L
umc44a	10.06	97.7	0.52	53.2	19.7	0.82	L
bnl7.49a(hmd)	10.07	114.1	0.73	63.8	21.1	0.91	L

Chromosome/SC number is indicated by the first number in the bin column. S, short; C, centromere; L, long.

[a] Micrometers from tip of short arm as predicted from the RN-cM map, except centromeres that are measured directly from SCs.